THE ASTROPHYSICAL JOURNAL, 319:662–670, 1987 August 15

H II REGION ABUNDANCES IN SEYFERT GALAXIES

I. N. EVANS AND M. A. DOPITA
Mount Stromlo and Siding Spring Observatories, The Australian National University
Received 1986 September 22; accepted 1987 February 2

ABSTRACT

The theoretical H II region abundance sequence calibration reported by Dopita and Evans in 1986 has been applied to optical spectrophotometry of 23 H II regions located in the inner disk regions of two Seyfert 1 and two Seyfert 2 galaxies, including the prototype Seyfert 2, NGC 1068, in order to determine oxygen, nitrogen, and sulfur abundances. The mean oxygen abundance derived for each galaxy ranges between solar abundance and twice solar abundance. There is no evidence for abnormal N/O or S/O abundance ratios in any of the H II regions we observed.

The observations suggest that the abundances derived for the H II regions may be adopted as nuclear abundances and employed to constrain theoretical models of the Seyfert nucleus. The observations then place limits on the influence which the active nucleus can have on chemical enrichment of the local interstellar medium.

Subject headings: galaxies: Seyfert — nebulae: abundances – nebulae: H II regions

I. INTRODUCTION

In recent years, considerable effort, both observational and theoretical, has been directed toward the study of active galactic nuclei in an attempt to understand the mechanism by which the nucleus is powered, and the effect of the nuclear activity on the surrounding galaxy. Many authors have computed theoretical photoionization and shock models for objects covering a range of nuclear activity from LINERs to the broad-line and narrow-line regions of Seyfert galaxies and quasars (see, for example, Kwan and Krolik 1981; Ferland and Netzer 1983; Halpern and Steiner 1983; Kwan 1984). In these models it has been frequently assumed *a priori* that the gas has a solar chemical composition, or approximately so, often with little or no observational basis for such an assumption. Since the most abundant elements (C, N, O, Ne) determine the line cooling in the gas, and in dense, hot regions where collisional ionization and Auger processes are significant may dominate the overall ionization balance, it is essential to employ accurate elemental abundances in order to correctly model the nuclear regions.

Because of uncertainties in physical processes and reddening corrections, it is not, in general, possible to estimate elemental abundances directly from observations of the nuclear spectrum except by way of self-consistency requirements for theoretical models. Hence, an alternate method for estimating the nuclear chemical composition must be sought. We propose that the most appropriate way of estimating nuclear elemental abundances is to adopt the abundances found in the galactic disk close to the nucleus, either from studies of near-nuclear H II regions (since such objects are more likely to have similar abundances to the nucleus due to their proximity than H II regions farther out in the disk), or, where such regions do not exist, from extrapolation of the radial abundance gradient to the nucleus. Although such a procedure will entrain its own uncertainties, nevertheless it should represent an improvement on the assumption of solar composition.

Comparison of abundances found in near-nuclear H II regions in Seyfert galaxies with those found in normal galaxies may also enable us to quantify any effects which the Seyfert nucleus may have upon chemical enrichment processes which occur in the interstellar medium (ISM). The most likely such effects are enhancement of the supernova rate and related nucleosynthetic processes triggered by compression of the ISM by winds, shock, and ionization fronts from the nucleus, and increased production of early-type stars in H II regions formed as a result of the high-level of turbulent activity near the nucleus. Bursts of star formation triggered by the nucleus may alter the relative enrichment of different elements in the ISM through modification of the stellar mass function.

In this paper we derive chemical abundances for 23 near-nuclear H II regions in two Seyfert 1 and two Seyfert 2 galaxies, including the prototypical Seyfert 2, NGC 1068. In § II we present our observational data set, from which we derive oxygen, nitrogen, and sulfur abundances in § III. In § IV, we discuss our reasons for believing that the H II region abundances we deduce may be adopted to constrain theoretical models of the Seyfert nuclei, and consider whether or not the high proton flux near the active nucleus may affect our abundance determinations by altering the ionization balance of near-nuclear H II regions. In § V we present our final conclusions.

II. OBSERVATIONS

The optical spectra were obtained under photometric conditions at the 3.9 m Anglo-Australian Telescope on the nights of 1983 May 11–12 and 12–13 (NGC 3783, NGC 4507, and NGC 6814), and on 1983 November 9–10 (NGC 1068). The Royal Greenwich Observatory spectrograph was used with the Image Photon Counting System (IPCS; Boksenberg 1972) as detector. A grating of 250 lines mm^{-1} blazed in the blue was used in first order with a slit width of 300 μm (2."01 on the sky), giving a spectral resolution of 8 Å and a spectral coverage of 3200–7400 Å. The external memory was formatted to give 64 spectra (96 spectra for the NGC 1068 observations), each 2040 pixels long, separated by 1."15 on the sky.

These spectra were reduced by the following procedure. First, pixel-to-pixel variations in the response of the detector were removed by division of the data by a normalized flat field obtained by summing two long exposures of an unfiltered tungsten lamp in third-order red. Second, each spectrum was rebinned to a linear wavelength scale by making a twodimensional third-order polynomial fit to the calibration arcs. Third, the mean of those spectra judged to be free of nebular or stellar contributions was subtracted from each spectrum to correct for night-sky emission. Fourth, the spectra were converted to absolute flux by correcting for extinction via observations of Oke (1974) white dwarf standard stars. Finally, the spectra of individual H II regions were obtained by co-adding all the spectra (or spatial increments) in which the object was detected.

The corrections for reddening applied to the observed fluxes were computed by assuming that the intrinsic Balmer decrement results from pure case B recombination (Brocklehurst 1971) for an adopted nebular temperature of 8000 K and employing the reddening curve of Seaton (1979). The spectra were first corrected for galactic extinction using the value of A_B tabulated by de Vaucouleurs, de Vaucouleurs, and Corwin (1976) for the line of sight to the parent galaxy. Next, the data were shifted to rest velocity and the observed ratio of $I(\mathrm{H}\alpha)/I(\mathrm{H}\beta)$ was used to determine the extragalactic extinction. The latter correction employed a "normal" galactic reddening law, since most of the extinction to extragalactic H II regions results from dust surrounding the nebula, rather than dust mixed with ionized gas (Brand, Coulson, and Zealey 1981; McCall, Rybski, and Shields 1985).

In some of the spectra the Balmer decrement steepens toward the series limit, indicating that a component of Balmer absorption is present. In the worst cases, the emission component of Hγ is annihilated. The Balmer absorption arises from both the underlying galaxy-disk continuum and the continuum due to the ionizing OB association in the H II region. To attempt to minimize the effect of the absorption on the emission-line intensity measurements, data from nearby spatial increments judged to be free of nebular contributions were summed together to form an average spectrum of the underlying continuum, and this spectrum was then scaled according to the shapes and intensities of prominent absorption features, and subtracted from the H II region data. The separation of the H II region emission spectrum from the underlying continuum is particularly difficult since in many cases the extent of the nebular emission implies that data from adjacent spatial increments cannot be used to estimate the continuum spectrum. Large point-to-point variations in the stellar age and the presence of A and B stars in the vicinity of the H II region, or a very strong but localized OB association continuum, means that the continuum subtracted is not identical to the continuum underlying the H II region spectrum. The most likely result is to overestimate the observed $I(\mathrm{H}\alpha)/I(\mathrm{H}\beta)$ emission-line ratio, and hence the reddening. This is evident in some of the spectra in Table 1 where $I(\mathrm{H}\gamma)$ is depressed relative to the theoretical value after the interstellar reddening has been removed on the basis of the observed $I(\mathrm{H}\alpha)/I(\mathrm{H}\beta)$ ratios. In such cases, caution needs to be applied when interpreting the data, but without additional high signal-to-noise spectrophotometry with both higher spectral and spatial resolutions, it is difficult to improve in these specific cases. However, *in general*, the technique is reasonably effective in removing the underlying absorption, but introduces increased uncertainties in the measured emission-line intensities, particularly for the higher order Balmer lines.

A further problem encountered when applying this procedure to NGC 1068 is the presence of weak optical emission over much of the inner disk region of the galaxy. The underlying emission was removed as far as possible before subtracting the averaged galaxy continuum spectrum from the H II region spectra, but this procedure has unavoidably introduced additional uncertainties in the measured intensities of the nebular emission lines, particularly for objects with low surface brightness. Nevertheless, the methods used should result in more reliable emission-line intensity measurements since, to first order, the effects of the underlying absorption have been reduced.

In Figure 1 we present a representative sky-subtracted and dereddened, but not continuum-subtracted, spectrum from an H II region in each of the four galaxies studied here. We

TABLE 1

OBSERVED (I_λ) AND REDDENING CORRECTED (F_λ) FLUXES

Ion	NGC 1068 (−018+009)		NGC 1068 (−022−009)		NGC 1068 (−027−033)		NGC 1068 (−029−038)		NGC 1068 (−031−049)		NGC 1068 (+023−016)		NGC 1068 (+027+048)		NGC 1068 (+024+032)	
	I_λ	F_λ	I_λ	F_λ	I_λ	F_λ	I_λ	F_λ	I_λ	F_λ	I_λ	F_λ	I_λ	F_λ	I_λ	F_λ
[Ne V] λ3426	...	...	...	...	...	...	...	...	...	...	...	...	...	...	99	308
[O II] λ3727	138	349	133	352	57	83	72	171	88	219	100	169	110	189	150	369
[Ne III] λ3868	...	...	...	...	...	...	...	...	...	...	...	...	...	...	...	...
He I, H7 λ3889	...	...	...	...	...	...	6.4	13.4	...	...	...	...	...	...	...	...
[Ne III], Hε λ3969	...	...	...	...	...	...	6.2	12.1	...	...	...	...	...	...	...	...
Hδ λ4102	...	...	...	...	...	...	13	24	...	...	...	...	...	...	...	...
Hγ λ4340	26	40	...	...	25	30	32	46	...	...	25	32	34	43	...	...
He II λ4686	...	...	...	...	...	...	...	...	...	...	...	...	...	...	26::	32::
Hβ λ4861	100		100		100		100		100		100		100		100	
[O III] λ4959	...	...	40	37	8.1	7.9	6.2	5.8	65	52	19	18	47	45	63	59
[O III] λ5007	92	83	90	81	20	19	23	21	150	136	35	33	151	142	135	122
[N I] λ5200	...	...	...	...	...	...	2.0:	1.6:	...	...	...	...	...	...	...	...
He I λ5876	11.2::	5.8::	...	...	6.0	4.6	14.1	7.6	...	...	...	...	...	...	...	...
[O I] λ6300	...	...	...	...	...	...	3.1::	1.4::	...	...	...	...	...	...	...	...
[N II] λ6548	156	56	158	55	56	36	124	48	142	52	68	38	110	61	144	54
Hα λ6563	817	291	857	291	447	291	765	291	805	291	523	291	531	291	791	291
[N II] λ6584	489	172	492	165	177	115	395	149	337	121	205	113	316	172	363	133
[S II] λ6716	134	44	124	39	46	29	67	24	105	35	65	35	80:	42:	100	34
[S II] λ6731	107	35	94	30	36	23	53	19	56	19	51	27	76:	40:	62:	21:
log F(Hβ)	−12.51		−12.33		−12.88		−12.26		−13.56		−13.10		−14.07		−13.14	
C(Hβ)	1.35		1.41		0.56		1.26		1.33		0.77		0.79		1.31	

TABLE 1—*Continued*

Ion	NGC 1068 (+022+021) I_λ	F_λ	NGC 1068 (+020+012) I_λ	F_λ	NGC 1068 (+019+004) I_λ	F_λ	NGC 1068 (+017−003) I_λ	F_λ	NGC 1068 (+011−036) I_λ	F_λ	NGC 3783 (+010−012) I_λ	F_λ	NGC 3783 (+004−014) I_λ	F_λ	NGC 3783 (+016−028) I_λ	F_λ
[Ne v] λ3426	96	225	9.4	18.1	32	81	18:	71:	...	...	...	...	...	...	...	...
[O II] λ3727	80	157	43	73	110	230	123	395	113	236	90	216	126	391	124	270
[Ne III] λ3868	11::	20::	2.5:	3.9:	18	34	11::	28::	...	...	...	...	...	...	...	...
He I, H7 λ3889	...	...	3.6	5.6	...	...	...	...	...	...	...	...	...	...	...	...
[Ne III], Hε λ3969 ..	...	...	7.1	10.6	...	...	...	...	...	...	...	...	...	...	...	...
Hδ λ4102	16	26	15	22	...	...	...	...	...	...	...	...	...	...	...	...
Hγ λ4340	28	37	33	42	17	24	21	34	28	39	22	33	15:	24:	...	...
He II λ4686	14:	17:	3.8	4.3	9.6:	11.4:	7.6::	9.8::	...	...	...	...	...	...	...	...
Hβ λ4861	100		100		100		100		100		100		100		100	
[O III] λ4959	57	54	15	14	81	77	70	65	15:	14:	...	...	...	...	...	...
[O III] λ5007	182	169	44	42	260	240	200	178	34	31	<7.7	<7.0	<12	<10	<19	<17
[N I] λ5200	...	...	3.5	3.1	...	...	...	...	...	...	...	...	...	...	...	...
He I λ5876	13.3::	8.2::	7.1	4.9	...	...	...	...	...	...	...	...	...	...	...	...
[O I] λ6300	...	...	4.1:	2.5:	...	...	...	...	...	...	...	...	...	...	...	...
[N II] λ6548	110	52	73	41	196	87	184	56	115	51	94	26	131	37	74::	31::
Hα λ6563	616	291	518	291	660	291	973	291	659	291	770	291	1036	291	690	291
[N II] λ6584	288	135	221	124	580	254	560	166	343	150	278	104	448	124	163	68
[S II] λ6716	79	35	55	30	160	67	140	38	82	34	118	42	188	48	65::	26::
[S II] λ6731	50	22	47	25	127	53	111	30	47	20	68	24	137	35	86::	34::
log F(Hβ)	−13.34		−12.28		−13.13		−12.48		−13.42		−13.85		−13.41		−14.46	
C(Hβ)	0.98		0.75		1.07		1.58		1.07		1.27		1.66		1.13	

TABLE 1—*Continued*

Ion	NGC 4507 (+001−019) I_λ	F_λ	NGC 4507 (−007−019) I_λ	F_λ	NGC 4507 (−013−018) I_λ	F_λ	NGC 4507 (−021−017) I_λ	F_λ	NGC 6814 (+016−016) I_λ	F_λ	NGC 6814 (+021−010) I_λ	F_λ	NGC 6814 (+027−002) I_λ	F_λ
[Ne v] λ3426	...	...	...	...	...	...	...	...	...	...	...	...	...	...
[O II] λ3727	191	389	138	292	168	327	168	319	<12	<37	23:	70:	17:	56:
[Ne III] λ3868	5.6:	10.4:	2.7::	5.2::	...	...	8.4:	14.7:	...	...	...	...	...	...
He I, H7 λ3889	...	...	...	...	...	...	...	...	...	...	...	...	...	...
[Ne III], Hε λ3969 ..	...	...	...	...	...	...	...	...	...	...	...	...	...	...
Hδ λ4102	...	...	...	...	12:	18:	...	...	...	...	...	...	...	...
Hγ λ4340	21	29	28	39	16	21	19	25	...	...	...	...	...	...
He II λ4686	...	...	...	...	...	...	...	...	...	...	...	...	...	...
Hβ λ4861	100		100		100		100		100		100		100	
[O III] λ4959	25	24	18	17	...	...	18	17	...	...	...	...	...	...
[O III] λ5007	58	54	47	44	25	23	45	42	<18	<16	<14	<12	<8.0	<7.0
[N I] λ5200	...	...	...	...	...	...	...	...	...	...	...	...	26	18
He I λ5876	...	...	13.4:	7.8:	...	...	...	...	...	...	...	...	...	...
[O I] λ6300	...	...	...	...	...	...	...	...	...	...	...	...	...	...
[N II] λ6548	104	48	82	36	91	44	85	42	75::	21::	194	57	147	39
Hα λ6563	642	291	674	291	613	291	597	291 1055	291	995	291	1111	291	
[N II] λ6584	255	115	252	108	254	120	244	118	154	42	323	94	362	94
[S II] λ6716	108	46	99	40	70	32	72	34	76::	19::	130	35	105	25
[S II] λ6731	68	29	78	32	55:	25:	43:	20:	59::	15::	89	24	44:	11:
log F(Hβ)	−13.53		−13.35		−13.98		−13.91		−13.72		−13.62		−13.23	
C(Hβ)	1.04		1.10		0.97		0.94		1.68		1.61		1.75	

employ the notation of McCall, Rybski, and Shields (1985) to identify and locate the H II regions observed. Observed (sky and galaxy continuum subtracted) and reddening-corrected emission-line intensities relative to $I(\mathrm{H}\beta) = 100$ are given in Table 1 for all the reduced H II region spectra. For each spectrum, we also list in Table 1 the absolute measured Hβ flux (corrected for extinction) and the logarithmic reddening constant at Hβ, $C(\mathrm{H}\beta)$, computed above.

III. H II REGION ABUNDANCES

For each of the H II regions listed in Table 1, we have estimated total oxygen, nitrogen, and sulfur abundances from the reddening-corrected emission-line ratios using the theoretical calibration of the extragalactic H II region abundance sequence by Dopita and Evans (1986), and employing the techniques suggested in that paper. The results of the abundance determinations from the sequence are shown in Table 2. Error estimates were computed in the following manner, as suggested by Evans (1986) which should be referred to for more detail. The uncertainty in the computed oxygen abundance was treated as a sum of two components: a "random" component, deduced from the consistency of the three different abundance estimators recommended by Dopita and Evans (1986); and a "systematic" component, resulting from possible differences between the actual nebular conditions and the nebular conditions adopted in the models used to calibrate the abundance

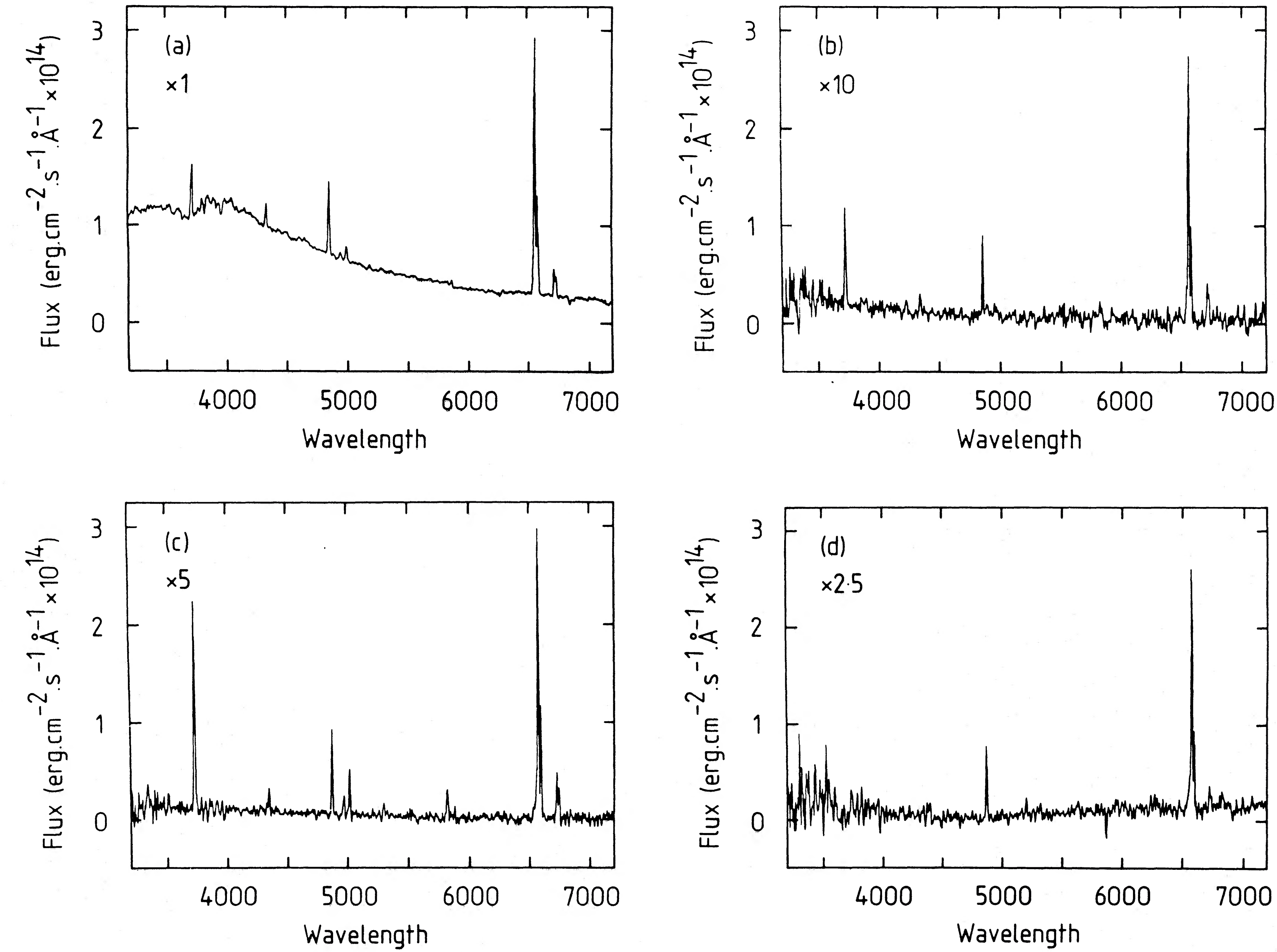

FIG. 1.—Representative spectra from H II regions in each of the four galaxies studied here. (*a*) NGC 1068 (−027 − 033), (*b*) NGC 3783 (−010 − 012), (*c*) NGC 4507 (+001 − 019), and (*d*) NGC 6814 (+027 − 002).

TABLE 2

ABUNDANCES DERIVED FROM THE ABUNDANCE SEQUENCE

Object	12 + log (O/H)	log (N/O)	log (S/O)
NGC 1068 (−018 + 009)......	8.76 ± 0.12	−0.75 ± 0.04	−1.33 ± 0.06
NGC 1068 (−022 − 009)......	8.74 ± 0.11	−0.76 ± 0.04	−1.46 ± 0.06
NGC 1068 (−027 − 033)......	9.07 ± 0.15	−0.79 ± 0.02	−1.54 ± 0.04
NGC 1068 (−029 − 038)......	8.98 ± 0.14	−0.80 ± 0.02	−1.61 ± 0.04
NGC 1068 (−031 − 049)......	8.89 ± 0.14	−0.92 ± 0.06	−1.61 ± 0.14
NGC 1068 (+023 − 016)......	8.97 ± 0.14	−0.91 ± 0.02	−1.53 ± 0.04
NGC 1068 (+027 + 048)......	8.91 ± 0.14	−0.78 ± 0.10	−1.48 ± 0.18
NGC 1068 (+024 + 032)......	8.69 ± 0.11	−0.82 ± 0.10	−1.50 ± 0.14
NGC 1068 (+022 + 021)......	8.95 ± 0.16	−0.86 ± 0.04	−1.58 ± 0.08
NGC 1068 (+020 + 012)......	9.08 ± 0.15	−0.75 ± 0.02	−1.52 ± 0.04
NGC 1068 (+019 + 004)......	8.83 ± 0.16	−0.62 ± 0.04	−1.41 ± 0.06
NGC 1068 (+017 − 003)......	8.64 ± 0.13[a]	−0.67 ± 0.12	−1.35 ± 0.32
NGC 1068 (+011 − 036)......	8.91 ± 0.13	−0.83 ± 0.06	−1.60 ± 0.14
NGC 3783 (+010 − 012)......	8.94 ± 0.13	−0.97 ± 0.06	−1.56 ± 0.10
NGC 3783 (+004 − 014)......	8.74 ± 0.14	−0.87 ± 0.06	−1.61 ± 0.12
NGC 3783 (+016 − 028)......	8.88 ± 0.13	−1.16 ± 0.16	−1.47 ± 0.24
NGC 4507 (+001 − 019)......	8.71 ± 0.12	−0.89 ± 0.02	−1.45 ± 0.12
NGC 4507 (−007 − 019)......	8.85 ± 0.12	−0.97 ± 0.02	−1.50 ± 0.04
NGC 4507 (−013 − 018)......	8.82 ± 0.13	−0.91 ± 0.04	−1.53 ± 0.12
NGC 4507 (−021 − 017)......	8.82 ± 0.12	−0.92 ± 0.04	−1.59 ± 0.14
NGC 6814 (+016 − 016)......	9.15 ± 0.16	−0.98 ± 0.36	−1.55 ± 0.50
NGC 6814 (+021 − 010)......	9.09 ± 0.15	−0.83 ± 0.18	−1.51 ± 0.26
NGC 6814 (+027 − 002)......	9.12 ± 0.15	−0.78 ± 0.18	−1.62 ± 0.30

[a] Derived from ([O II] λ3727 + [O III] $\lambda\lambda$4959,5007)/Hβ only.

sequence. The latter were estimated not to exceed ±0.15 dex for 12 + log (O/H) = 9.1 decreasing linearly to ± 0.05 dex for 12 + log (O/H) = 8.2 Evans 1986). It should be emphasized that the sytematic errors dominate for high oxygen abundances, and that they are not standard errors, but rather their meaning is that it is extremely unlikely that the difference between the actual nebular abundances and the calculated abundances will exceed the stated errors. The uncertainty in the N/O ratio, which is less temperature sensitive than the ratios of either element alone with respect to hydrogen, is generally less than the uncertainty in the O/H ratio and arises mainly from uncertainties in the measured line intensities. Likewise, the uncertainty in the S/O ratio arises primarily from uncertainties in the measured line intensities, although in this case there is also a contribution which arises from the strong dependence of the intensity of the [S II] λ6731 emission line on the ionization parameter [$\bar{Q}$(H), defined by Evans and Dopita 1985].

We derive the mean oxygen, nitrogen, and sulfur abundances for the inner disk region of each galaxy from the H II region observations separately below.

a) NGC 1068

We have estimated elemental abundances in 13 H II regions observed in the prototype Seyfert 2 galaxy NGC 1068 covering the range of radii 20″–60″ from the nucleus. This sample is sufficient to enable us to establish whether or not a strong radial abundance gradient is present in the inner disk region of this galaxy. The true radial distance of each H II region to the nucleus of the galaxy projected onto the plane of the galactic disk was computed from the apparent radial distance assuming that the position angle of the major axis of the galaxy is 52° (Nishimura, Kaneko, and Toyama 1984) and that the inclination of the galactic disk to the line of sight is given by sec i = 1.18 (de Vaucouleurs, de Vaucouleurs, and Corwin 1976). The adopted isophotal radius of NGC 1068 is taken to be R_0 = 3′32″ = 11.68 kpc, and the adopted distance (H_0 = $100h^{-1}$ km s^{-1} Mpc^{-1}) is 11.34h kpc (de Vaucouleurs, de Vaucouleurs, and Corwin 1976).

In Figure 2 we plot the oxygen abundance derived for each H II region versus its fractional isophotal radius, ρ. A first inspection of the figure suggests that there is no clear evidence for a radial gradient in oxygen abundance for the sample of H II regions which we observed, and that considerable scatter in oxygen abundance from region to region is evident. However, it is well established that weak [O III] $\lambda\lambda$4959, 5007 emission extends over much of the inner disk region of NGC 1068 (Burbidge, Burbidge, and Prendergast 1958; Bertola 1968; Walker 1968; Balick and Heckman 1979) extending out as far as 50″ from the nucleus along the major axis of the galaxy (Nishimura, Kaneko, and Toyama 1984).

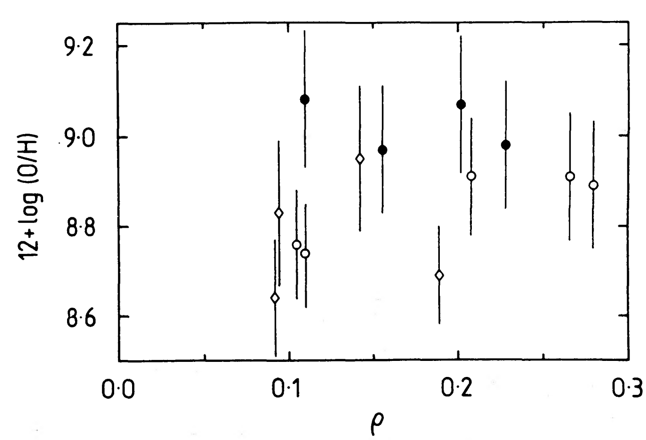

FIG. 2.—The oxygen abundances derived for the H II regions in NGC 1068 plotted against fractional isophotal radius, ρ. The filled circles represent those regions with $S_{H\beta} > 5 \times 10^{-16}$ ergs cm^{-2} s^{-1} arcsec^{-2}, while the open circles indicate those regions with lower mean surface brightnesses likely to be affected by the underlying disk emission. The diamonds locate H II regions whose spectra are likely to be affected by the high-excitation emission to the NE of the nucleus.

In addition, we detect extended emission from other lines. The cause of this weak extended emission is not well established, but may be due to absorption of low-energy X-ray photons emitted from the Seyfert nucleus by warm ($\sim 10^4$ K) interstellar clouds (Evans and Dopita 1986). The excess line-emission arising from the underlying component, together with the increased uncertainties resulting from the subtraction of the averaged disk absorption spectrum, significantly increase the total uncertainties in the measured emission-line ratios (and hence abundance estimates) for H II regions with low surface brightness. The excess line-emission emanating from the underlying component results in an underestimate of the oxygen abundance for those objects with *relatively* strong background emission. On the basis of the signal-to-noise ratios of the observed spectra, we estimate that this effect is unimportant for objects with a mean apparent Hβ surface brightness greater than $\sim 5 \times 10^{-16}$ ergs cm^{-2} s^{-1} arcsec^{-2} and becomes increasingly important with decreasing surface brightness. In Figure 2, H II regions which have $S_{\mathrm{H}\beta} > 5 \times 10^{-16}$ ergs cm^{-2} s^{-1} arcsec^{-2} are indicated by filled circles, while those with lower $S_{\mathrm{H}\beta}$ are marked with open circles. A further complication is the presence of an extended region of high-excitation emission to the NE of the nucleus. This region shows strong lines of [Ne V] $\lambda\lambda$3346, 3426 and also He II λ4686 superposed on normal H II region spectra and has been interpreted as emission from ordinary H II regions superposed on emission from a region photoionized by a power-law X-ray spectrum emanating from the Seyfert nucleus (Evans and Dopita 1986). The theoretical photoionization models presented in that paper suggest that the high-excitation region can contribute a considerable fraction of the total [O III] $\lambda\lambda$4959, 5007 emission observed. Diamonds are used in Figure 2 to indicate H II regions likely to be significantly affected by this emission. If we consider only those H II regions unlikely to be affected by either of the above complicating factors (the filled circles in Fig. 2), we find no evidence for a radial gradient in oxygen abundance over the range of ρ observed, and estimate the mean oxygen abundance to be $12 + \log(\mathrm{O/H}) = 9.02 \pm 0.07$, with only a small amount of scatter.

For the same H II regions used to derive the mean oxygen abundance, we deduce mean nitrogen to oxygen and sulfur to oxygen ratios of $\log(\mathrm{N/O}) = -0.81 \pm 0.07$ and $\log(\mathrm{S/O}) = -1.55 \pm 0.04$, respectively. These values are comparable to the solar values (Allen 1973), $\log(\mathrm{N/O}) = -0.86$ and $\log(\mathrm{S/O}) = -1.62$, indicating that neither element is over-abundant relative to oxygen, but that oxygen is mildly over-abundant by (0.2 dex) relative to the solar value in the inner H II regions of NGC 1068.

b) NGC 3783

Three H II regions were observed in the Seyfert 1 galaxy NGC 3783. Two of the H II regions were situated $\sim 15''$ from the nucleus in the inner ring of this theta-type barred spiral near the southern end of the bar, while the third H II region was located at approximately twice the radius of the other two in a spiral arm SW of the nucleus. Compared to the H II regions in NGC 1068, the H II regions in NGC 3783 have much lower mean surface brightnesses. Consequently, our spectra of these objects have somewhat lower signal-to-noise ratios. Combined with the apparently lower degree of excitation found in these H II regions (e.g., Fig. 1) this implies that only upper limits could be established for the intensity of [O III] λ5007 in each case. However, [O II] λ3727 was readily detected, as were the other lines necessary to derive an abundance estimate. The abundances computed using the upper limits for the [O III] λ5007 line intensities did not deviate either consistently or significantly from those made with estimators not employing the [O III] λ5007 line. Hence we have confidence that our abundance estimates for these objects are not biased by the lack of a positive detection of this line.

The mean oxygen abundance derived from the three H II regions is given by $12 + \log(\mathrm{O/H}) = 8.86 \pm 0.08$. There are insufficient data for this galaxy to establish whether or not a radial gradient exists, but the morphology of the galaxy argues strongly against the presence of a steep abundance gradient since the bar-forming potential in the stellar disk of the galaxy is expected to produce considerable radial mixing of the ISM (Schwarz 1981; see also § IV below). The mean nitrogen to oxygen abundance ratio for the three H II regions is $\log(\mathrm{N/O}) = -1.00 \pm 0.15$, while the mean sulfur to oxygen ratio is $\log(\mathrm{S/O}) = -1.54 \pm 0.10$. Within the errors the oxygen, nitrogen, and sulfur abundances in the H II regions we observed are neither underabundant nor overabundant compared to the solar values.

c) NGC 4507

For the Seyfert 2 galaxy NGC 4507, four H II regions were observed with galactocentric radii between 19″ and 26″. As for NGC 3783 and NGC 6814 (§ III*d* below), the limited range of galactocentric radii makes it impossible for us to derive an abundance gradient from these data. Only mean abundances can be determined. Inspection of the representative spectrum shown in Figure 1 indicates that the H II regions we observed in this galaxy have the lowest mean oxygen abundance of our sample, and, as expected since the ionization parameter and oxygen abundance are inversely correlated (Dopita and Evans 1986), high excitation. The abundances derived from the sequence confirm the qualitative results suggested by the figure, and we derive a mean oxygen abundance from the observations of $12 + \log(\mathrm{O/H}) = 8.80 \pm 0.06$, with N/O and S/O ratios given by $\log(\mathrm{N/O}) = -0.92 \pm 0.02$ and $\log(\mathrm{S/O}) = -1.53 \pm 0.02$, respectively. Even though these H II regions represent the lowest mean abundances in our sample, we note that they are not significantly lower than the solar values.

d) NGC 6814

Three H II regions were observed in the Seyfert 1 galaxy NGC 6814, covering a range of galactocentric radii between 23″ and 27″. It is immediately apparent from the weakness of the forbidden lines (e.g., Fig. 1) that the three H II regions have a considerably higher than solar oxygen abundance and a very low ionization parameter. Indeed, in the case of NGC 6814 (+027−002), there is a clear detection of the low excitation [N I] $\lambda\lambda$5198, 5201 doublet which is emitted in the hydrogen transition zone where a significant fraction of neutral hydrogen exists. For each spectrum, only upper limits for the intensities of the [O III] λ5007 line could be established, and in one case only an upper limit could be set for the intensity of [O II] λ3727 while for the other objects the detection was marginal (2–3 σ). Even so, the good agreement found between the oxygen abundance determinations computed using the three different estimators recommended by Dopita and Evans (1986), for each of the H II regions, gives us confidence in the values derived. We find a mean oxygen abundance given by $12 + \log(\mathrm{O/H}) = 9.12 \pm 0.09$, which is a factor of 2 larger than the solar value, and is 0.24 dex higher than the oxygen abundance measured in the high-abundance H II region S5 in M101 (Evans 1986). On the other hand, the relative abundances of nitrogen and sulfur to oxygen are more typically solar, with values of log (N/O) $= -0.86 \pm 0.06$ and log (S/O) $= -1.56 \pm 0.03$, respectively.

IV. DISCUSSION

The results presented in the previous section suggest that the abundances of the elements oxygen, nitrogen, and sulfur present in the inner regions of the Seyfert galaxies which we studied are typically solar, or perhaps somewhat overabundant with respect to solar. None of the H II regions in the four galaxies studied show any evidence for oxygen abundances significantly lower than solar, and this is also true for other Seyfert galaxies for which abundance measurements in H II regions have been conducted (e.g., Pagel *et al.* 1979; Hawley and Phillips 1980).

The lack of any evidence to suggest that N/O or S/O abundance ratios are abnormal in any of the H II regions in our sample indicates that preferential enrichment or depletion of these elements relative to oxygen cannot be important in the inner disk regions of the galaxies we observed. This suggests, for example, that enhancements of the supernova or star-formation rates and related nucleosynthetic processes triggered by nuclear shocks and winds compressing the local ISM are either too insignificant to effect the overall chemical enrichment of inner disk, or that such processes do not greatly modify the local stellar mass function over the timescale of the nuclear activity. With the advent of Space Telescope, it should be possible to discriminate between these possibilities by a program of spatially resolved spectrophotometry of the nuclear regions.

Whether or not a direct correlation exists between elemental abundances and Seyfert activity is both uncertain and difficult to establish. There is evidence to suggest that Seyfert galaxies occur with only a narrow range of morphological types. Sérsic (1973) pointed out that many Seyferts tend to be barred spirals, while de Vaucouleurs (1974) noted that Seyfert galaxies tend to have Hubble types earlier than Sbc, and Adams (1977) indicated that many Seyferts have ring structures. Simkin, Su, and Schwarz (1980) have constructed theoretical disk models which reproduce the range of morphological types observed, and suggest that they may form an evolutionary sequence. In particular, correlations are observed between morphological type parameterized by age along the theoretical evolutionary sequence and quantities, such as the FWZI of the Balmer lines or the X-ray luminosity, characterizing the degree of activity for Seyfert 1 nuclei (Su and Simkin 1980). At the same time, it is well known that irregular galaxies and late-type spirals tend to contain H II regions with low metal abundances, and that metallicity tends to increase as one progresses from late-type galaxies to early-type galaxies, and with increasing luminosity. Hence it is certainly possible that the limited range of metal abundances seen in Seyfert galaxies is due only to the correlation of metal abundance with galaxy morphology and the restricted range of morphological types occupied by Seyfert galaxies but is causally unrelated in any way to the Seyfert activity itself.

More significant for models of Seyfert galaxies and their nuclei is the apparent lack of strong radial abundance gradients. Our data for NGC 1068 suggest that no obvious gradient in metal abundance is present in this galaxy, at least in the inner region of the disk over which our observations range. Likewise, there is no evidence for large abundance gradients in the Seyfert galaxies NGC 1365 (Pagel *et al.* 1979) and NGC 1566 (Hawley and Phillips 1980) which have well-studied H II regions. Furthermore, neither of the active galaxies M51 and M83 show evidence for large abundance gradients. The former galaxy exhibits "Seyfert-like" nuclear activity (Rose and Searle 1982; Rose and Cecil 1983), and there are indications of active sites situated outside the nucleus possibly originating from a bi-directional nuclear jet (Ford *et al.* 1985). The latter galaxy has been classified as having a starburst nucleus (Bohlin *et al.* 1983). On the other hand, we find that abundance gradients tend to be quite pronounced in late-type spirals, such as M33 (Dopita, D'Odorico, and Benvenuti 1980) and M101 (Evans 1986), which do not exhibit strong nuclear activity.

The lack of steep abundance gradients in Seyfert galaxies is almost certainly related to their limited range of morphologies, following the suggestion of Searle (1971) and Smith (1975) that a correlation exists between abundance gradients and morphological type. One reason for such a correlation has been suggested by Schwarz (1979, 1981) who demonstrated that in a gravitational potential produced by a stellar background with a sharply peaked central density distribution, a rotating gaseous disk would develop a sequence of spiral and then ring-like patterns when perturbed by a rotating 2θ potential with the appropriate pattern speed. Su and Simkin (1980) showed that the range of morphologies observed for Seyfert galaxies were well fitted by the theoretical disk model. As the model sequence evolved, the gas in the inner regions of the disk developed a strong flow into the nuclear regions on a time scale short compared with the age of the galaxy. Models with radial inflow of gas are also required to adequately explain observed abundance gradients in normal spiral galaxies (e.g., Tinsley and Larson 1978; Mayor and Vigroux 1981; Lacey and Fall 1985) and are expected to be present in most galaxy disks. When combined with the outflow of material from the active nucleus, predicted by a number of models (e.g., Kippenhahn, Mestel, and Perry 1975; Blandford and Königl 1979; Krolik and Vrtilek 1984) and observed in some cases (e.g., Cecil and Rose 1984; Heckman, Miley, and Green 1984; Wamsteker and Barr 1985), this implies that substantial radial mixing of the ISM must take place in the inner regions of the disk, minimizing the formation of abundance gradients and possibly also enhancing star formation through turbulent motions and compression. A major consequence of the radial mixing predicted by such models is that the chemical composition of the gas which makes up the narrow-line region, and possibly also the broad-line region, will be similar to the chemical composition to the H II regions found in the inner disk. Hence, measurements of elemental abundances in near-nuclear H II regions may be used to constrain theoretical models of the active nuclear regions.

Let us now consider whether the high ionizing luminosity of the active nucleus may affect the gas in near-nuclear H II regions. At small radii from the nucleus, it seems highly probable that the intense photon flux from the nuclear ionizing spectrum would either dominate or at least significantly alter the ionization balance in an H II region, unless the latter is somehow shielded from the central source. Large changes in the ionization balance of H II regions arising from the nuclear ionizing photon flux would almost certainly render invalid abundance determinations from those objects. Besides directly altering the ionization balance within the H II regions, the nuclear spectrum may ionize the lower density interstellar medium and clouds surrounding them. An example of this is NGC 1068, where both high-excitation emission is seen superposed with H II region spectra to the NE of the nucleus (Evans and Dopita 1986), and low-level underlying emission is observed over much of the inner 2–3 kpc of the disk. The radius within the disk to which such effects may be important depends upon the shape of the ionizing spectrum and the ionizing luminosity of the central source, and the column density and absorption cross section of the intervening material. Assuming isotropic emission from the nuclear photon source, and a uniformly dense interstellar medium we can estimate the radius in the disk at which the nuclear photon source should have negligible effect on the ionization balance in the H II regions as follows. The ionization parameter due to the central source, at any radius r from the nucleus, is given by

$$Q(H, r) = L_C/4\pi r^2 N ,$$

where L_C is the ionizing photon luminosity and N is the number density of atoms plus ions for the intervening material. The lowest value of the ionization parameter is low-excitation (metal-rich) H II regions is $\sim 5 \times 10^6$ cm s^{-1} (Dopita and Evans 1986), so if we assume that a value of $Q(H, r) = 2 \times 10^6$ cm s^{-1} represents a level where the ionization due to the nuclear source is insignificant relative to the local ionization due to the OB association illuminating the H II region, and taking $N = 0.3$ cm^{-3} as being representative of the intervening interstellar medium in the disk, we find

$$r_{\max} \approx 2.7 L_{42}{}^{1/2} \text{ kpc} ,$$

where $r_{\max}$ is the radius at which the ionization parameter declines to 2×10^6 cm s^{-1}, L_{42} is the 0.5–4.5 keV X-ray luminosity in units of 10^{42} ergs s^{-1}, and we have assumed for simplicity that the nuclear ionizing spectrum can be represented as a power-law, $F_\nu \propto \nu^\alpha$, with spectral index $\alpha = -1$. For example, for NGC 1068 where the 0.5–4.5 keV X-ray luminosity is $\sim 7.2 \times 10^{41}$ ergs s^{-1} (Lawrence and Elvis 1982), we find $r_{\max} \approx 2.3$ kpc, which is in good agreement with the extent of the underlying disk emission in that galaxy. The presence of density inhomogeneities, such as interstellar or molecular clouds, or regions of low-density coronal gas in pressure equilibrium with the interstellar medium expected to exist in the strong X-ray fields of active galactic nuclei (Lepp *et al.* 1985), will alter $r_{\max}$, but the above expression gives an approximate estimate for the extent of the nuclear influence. When attempting to derive abundances from H II regions with radii $r \lesssim r_{\max}$ one should be appropriately cautious, although the increased number density within the H II region will considerably reduce the effective ionization parameter of the nuclear spectrum relative to the input value at the edge of the H II region. For H II regions with $r \approx r_{\max}$ the most likely effects of the nuclear spectrum will be increased emission from low ionization species which exist in the hydrogen transition zone at the edge of the nebula and contamination of the pure H II spectrum by emission from the lower density warm ISM surrounding the region.

V. CONCLUSIONS

We have applied the theoretical abundance sequence calibration of Dopita and Evans (1986) to low resolution spectrophotometry of 23 H II regions in two Seyfert 1 and two Seyfert 2 galaxies in order to estimate elemental abundances. The mean oxygen abundance derived from the H II region observations in each galaxy ranges from approximately solar abundance to twice solar abundance. In all cases we find that the ratios of nitrogen abundance and sulfur abundance to oxygen abundance are about the same as the solar values, indicating that these elements are not preferentially enriched or depleted relative to oxygen. This implies that processes excited by the nuclear activity which would result in preferential chemical enrichment have not been a significant factor in determining the local chemical composition of the ISM.

The absence of a steep abundance gradient in the inner regions of NGC 1068, combined with similar results for other Seyfert and active galaxies, suggests that substantial radial mixing of the ISM has occurred in the inner disks of these galaxies. It therefore seems possible that elemental abundances found in near-nuclear H II regions could be adopted as nuclear abundances as a constraint on theoretical models for the narrow-line and broad-line regions of the Seyfert nucleus. It is somewhat fortuitous that the abundances we measure are approximately solar, or slightly higher, since the majority of theoretical models which have to date been reasonably successful in explaining the emission-line intensities and continua emitted by Seyfert and other active nuclei have often, *a priori*, assumed a solar abundance set.

For H II regions lying within a few kpc of the nucleus, the influence of the nuclear ionizing spectrum on the ionization balance should be taken into account when interpreting the spectra of the H II regions to derive elemental abundances. The most likely effect of the nuclear luminosity is to increase the forbidden line emission, resulting in artificially low abundance estimates for very near-nuclear H II regions. This effect is in fact evident in the data for the H II regions in NGC 1068 with very small fractional radii.

The overabundance of the elements, and the relatively small range of abundances displayed by our sample of galaxies, is an interesting result that needs confirmation in a larger sample of Seyfert and other active galaxies. In addition, further theoretical studies of the chemical and dynamical evolution of the nuclear regions are required to establish whether or not there is a causal relationship between strong radial flows and mixing of the local ISM near the nucleus and the nuclear activity. For example, one can envisage that the gas close to the nucleus could behave as a relaxation oscillator. Strong radial flows to the nucleus could give rise to starburst activity through compression of the ISM, and the formation of a nuclear accretion disk. The increasing activity and turbulence may result in the formation of a Seyfert nucleus and an outflowing nuclear wind. The latter may eventually dissipate the circumnuclear gas and cut off the nuclear activity, after which a new radial flow could result, thus repeating the process.

One of us (I. N. E.) acknowledges the receipt of an Australian Commonwealth Postgraduate Research Award.

REFERENCES

Adams, T. F. 1977, *Ap. J. Suppl.*, **33**, 19.
Allen, C. W. 1973, *Astrophysical Quantities* (3d ed.; London: Athlone).
Balick, B., and Heckman, T. M. 1979, *A.J.*, **84**, 302.
Bertola, F. 1968, *A.J.*, **73**, 861.
Blandford, R. D., and Königl, A. 1979, *Ap. Letters*, **20**, 15.
Bohlin, R. C., Cornett, R. H., Hill, J. K., Smith, A. M., and Stecher, T. P. 1983, *Ap. J. (Letters)*, **274**, L53.
Boksenberg, A. 1972, in *Proc. ESO/CERN Conference on Auxiliary Instrumentation for Large Telescopes*, ed. S. Laustsen and A. Reiz (Geneva: CERN), p. 295.
Brand, P. W. J. L., Coulson, I. M., and Zealey, W. J. 1981, *M.N.R.A.S.*, **195**, 353.
Brocklehurst, M. 1971, *M.N.R.A.S.*, **153**, 471.
Cecil, G., and Rose, J. A. 1984, *Ap. J.*, **287**, 131.
de Vaucouleurs, G. 1974, in *IAU Symposium 58, Formation and Dynamics of Galaxies*, ed. J. R. Shakeshaft (Dordrecht: Reidel), p. 332.
de Vaucouleurs, G., de Vaucouleurs, A., and Corwin, H. G. 1976, *Second Reference Catalogue of Bright Galaxies* (Austin: University of Texas).
Dopita, M. A., D'Odorico, S., and Benvenuti, P. 1980, **236**, 628.
Dopita, M. A., and Evans, I. N. 1986, *Ap. J.*, **307**, 431.
Evans, I. N. 1986, *Ap. J.*, **309**, 544.
Evans, I. N., and Dopita, M. A. 1985, *Ap. J. Suppl.*, **58**, 125.
———. 1986, *Ap. J. (Letters)*, **310**, L15.
Ferland, G. J., and Netzer, H. 1983, *Ap. J.*, **264**, 105.
Ford, H., Crane, P., Jacoby, G., Lawrie, D., and van der Hulst, J. M. 1985, *Ap. J.*, **293**, 132.
Halpern, J. P., and Steiner, J. E. 1983, *Ap. J. (Letters)*, **269**, L37.
Hawley, S. A., and Phillips, M. M. 1980, *Ap. J.*, **235**, 783.
Heckman, T. M., Miley, G. K., and Green, R. F. 1984, *Ap. J.*, **281**, 525.
Kippenhahn, R., Mestel, L., and Perry, J. J. 1975, *Astr. Ap.*, **44**, 123.
Krolik, J. H., and Vrtilek, J. M. 1984, *Ap. J.*, **279**, 521.
Kwan, J. 1984, *Ap. J.*, **283**, 70.
Kwan, J. and Krolik, J. H. 1981, *Ap. J.*, **250**, 478.
Lacey, C. G., and Fall, S. M. 1985, *Ap. J.*, **290**, 154.
Lawrence, A., and Elvis, M. 1982, *Ap. J.*, **256**, 410.
Lepp, S., McCray, R., Shull, J. M., Woods, D. T., and Kallman, T. 1985, *Ap. J.*, **288**, 58.
Mayor, M., and Vigroux, L. 1981, *Astr. Ap.*, **98**, 1.
McCall, M. L., Rybski, P. M., and Shields, G. A. 1985, *Ap. J. Suppl.*, **57**, 1.
Nishimura, M., Kaneko, N., and Toyama, K. 1984, *Astr. Ap.*, **130**, 46.
Oke, J. B. 1974, *Ap. J. Suppl.*, **27**, 21.
Pagel, B. E. J., Edmunds, M. G., Blackwell, D. E., Chun, M. S., and Smith, G. 1979, *M.N.R.A.S.*, **189**, 95.
Rose, J. A., and Cecil, G. 1983, *Ap. J.*, **266**, 531.
Rose, J. A., and Searle, L. 1982, *Ap. J.*, **253**, 556.
Schwarz, M. P. 1979, Ph.D. thesis, Australian National University.
———. 1981, *Ap. J.*, **247**, 77.
Searle, L. 1971, *Ap. J.*, **168**, 327.
Seaton, M. J. 1979, *M.N.R.A.S.*, **187**, 73P.
Sérsic, J. L. 1973, *Pub. A.S.P.*, **85**, 103.
Simkin, S. M., Su, H. J., and Schwarz, M. P. 1980, *Ap. J.*, **237**, 404.
Smith, H. E. 1975, *Ap. J.*, **199**, 591.
Su, H. J., and Simkin, S. M. 1980, *Ap. J. (Letters)*, **238**, L1.
Tinsley, B. M., and Larson, R. B. 1978, *Ap. J.*, **221**, 554.
Walker, M. F. 1968, *Ap. J.*, **151**, 71.
Wamsteker, W., and Barr, P. 1985, *Ap. J. (Letters)*, **292**, L45.

MICHAEL A. DOPITA and IAN N. EVANS: Mount Stromlo and Siding Spring Observatories, Private Bag, Woden P.O., ACT 2606, Australia